Microphase separation of diblock copolymers with amphiphilic segment

Kriksin, Yury A.; Khalatur, Pavel G.; Erukhimovich, Igor Ya.; ten Brinke, Gerrit; Khokhlov, Alexei R.

Published in:
Soft Matter

DOI:
10.1039/b905923g

Publication date:
2009

Microphase separation of diblock copolymers with amphiphilic segment

Yury A. Kriksin,[a] Pavel G. Khalatur,*[bc] Igor Ya. Erukhimovich,[c] Gerrit ten Brinke[d] and Alexei R. Khokhlov[bce]

Received 25th March 2009, Accepted 29th April 2009
First published as an Advance Article on the web 10th June 2009
DOI: 10.1039/b905923g

We present a statistical mechanical approach for predicting the self-assembled morphologies of amphiphilic diblock copolymers in the melt. We introduce two conformationally asymmetric linear copolymer models with a local structural asymmetry, one of a "comb-tail" type and another that we call "continuous jackknife model." The copolymers consist of amphiphilic and "monophilic" (non-amphiphilic) blocks, which have different segmental volume and tend to segregate into subphases. Using a self-consistent field theory (SCFT) framework, we explore the phase diagrams for these copolymers and compare them with that known for conventional, conformationally symmetric diblock copolymers. To determine the impact of structural effects on the self-assembly of copolymer melts, copolymers with a variation in both molecular architecture and chemical composition, f, are studied for different values of the Flory–Huggins parameter, χ. The composition dependence of the phase diagrams is shown to be basically determined by the conformational asymmetry. Remarkably, the stable lamellar structures exist even in the very compositionally asymmetric case, $f < 1/4$. An interesting geometric distinction of the "direct" and "inverse" morphologies is introduced. The presence of an internal structure is found to influence the high χ behavior, where a stable two-scale (structure-in-structure) hexagonal morphology is found to be formed for some compositions. Therefore, the local chemical structure of monomer units can dictate the global morphology of copolymer melts.

1. Introduction

Microphase segregated copolymer melts and solids have long garnered significant scientific interest due to their ability to spontaneously form periodic morphologies at controllable length scales.[1–5] Self-assembly is also one of the most universal strategies used in biology for the development of complex and functional (nano)structures: fascinating examples are multimeric proteins and nucleic acid multiplexes, viruses, and biomembranes. Such systems have been extensively studied over the years, to allow for a better understanding of their structure and functions.

The A_f-b-B_{1-f} diblock architecture provides the simplest model for examining microphase separation in monodisperse copolymer melts. The block copolymers are structures formed by at least two chemically different polymer chains, A and B, linked together by a covalent bond. The microphase separation is governed by the chemical composition (the fraction f of segments that belong to, *e.g.*, the A block) and the product of Flory–Huggins interaction parameter χ of the copolymer segments and the total number of segments per chain, N. The physical reason for copolymer self-assembly, which is also called microphase separation or order–disorder transition (ODT), is obvious: with increasing the segregation strength χN, the energy gain from local segregation grows as compared to the loss of the translational entropy accompanying such segregation, while the immiscible A and B blocks can not separate fully because of their covalent connection. As a result, an ordered pattern of alternating domains filled preferably with segments of the same sort arises.

The theory of microphase separation in diblock copolymers has been developed in detail and this subject has been reviewed extensively.[1–9] In particular, a phase diagram, which shows the regions of stability of the morphologies of various symmetry, was predicted[6–10] for diblock copolymer melts. These morphologies, with length scales of the order of 1 to 10^2 nm, may be controlled by changing the lengths of blocks, the proportions of A and B monomeric units, or the interaction between them.

More complicated structures are achieved for multiblock copolymers or if more blocks or different architectures, such as star-shape (mictoarm) or dendritic shapes copolymers, are used.[11,12] The recent studies of the so-called *two-length-scale* multiblock copolymer systems $[A_{mN}(B_{N/2}A_{N/2})_n$ and $A_{fmN}(B_{N/2}A_{N/2})_nB_{(1-f)mN}$, where n and m are integers][13–16] showed that their microphase segregation behavior is far from that of a diblock copolymer melt. For these copolymers, non-conventional sequences of the order–order transitions were predicted within the week segregation theory (WST)[14,17] and self-consistent field theory (SCFT).[16] For instance, Kriksin *et al.*[16] have recently demonstrated that the set of stable morphologies for linear copolymers with the multiblock architecture $A_{fmN}(B_{N/2}A_{N/2})_n$-$B_{(1-f)mN}$ differs from that known for simple diblock melts, where longer and shorter blocks form the matrix and micelles, respectively. On the contrary, for the former the longer end blocks B tend to segregate into the micelles whereas the shorter block A and the middle multiblock part form together the matrix. The phase diagram involving these *inverse morphologies* was

[a]*Institute for Mathematical Modeling, RAS, Moscow, 125047, Russia*
[b]*Department of Polymer Science, University of Ulm, Ulm, D-89069, Germany. E-mail: khalatur@germany.ru*
[c]*Institute of Organoelement Compounds, RAS, Moscow, 119991, Russia*
[d]*Laboratory of Polymer Chemistry, Zernike Institute for Advanced Materials, University of Groningen, Nijenborgh 4, 9747 AG Groningen, The Netherlands*
[e]*Physics Department, Moscow State University, Moscow, 119899, Russia*

calculated in that region of the system parameters, where segregation inside the middle multiblock part $(B_{N/2}–b–A_{N/2})_n$ does not occur yet, and turned out to be similar to that of ternary linear ABC block copolymers.[17]

Other examples of self-assembled polymeric structures are comb-shaped supramolecules, where low-molecular-weight compounds (*e.g.*, small amphiphilic molecules) are attached to polymer backbone by physical interactions instead of covalent bonding.[17–21] In these systems, structure formation and phase behavior are mainly affected by the attraction strength of the polymer–amphiphile interaction and repulsion between the polar polymer backbone and non-polar tails.[18–21]

It should be stressed that in most of the theoretical studies it is assumed that the polymer blocks are conformationally symmetric; that is, they have equal Kuhn segment length, ℓ, and segmental volume, v.[6–9] The conformational asymmetry can cause considerable changes in the phase diagrams, *e.g.*, by introducing only a slight difference in either the statistical segment lengths and/or segmental volumes between the constituents of a diblock, such as in the often studied system of polystyrene and polyisoprene, the microphase boundaries become asymmetric about $f = ½$.[22–24] Matsen and Bates found that for copolymers with a stiff minority block, conformational asymmetry stabilizes the gyroid (G) phase, widening the composition window and moving the lamellar-G and G-cylinder boundaries to higher stiff compositions.[24] On the other hand, the presence of a stiff majority block destabilizes the G phase. The thermodynamic implications of conformational asymmetry between the two blocks of diblock copolymers are considered to explain a lot of experimental results.[25,26]

It is a commonplace to say that the properties of a copolymer depend not only on its global architecture and chemical composition but also on the *local chemical structure* of its monomeric units. Therefore, an important route in the precise control and theoretical prediction of molecular parameters required to achieve well-defined microphase-separated morphologies is connected with understanding the role of local polymer structure responsible for intra- and intermolecular interaction.

The drawback of the existing field-theoretical approaches based on the standard Gaussian chain model is the representation of each monomeric unit of a real polymer as a point-like interaction site of pure repulsive or pure attractive type. At the same time, in the large majority of real heteropolymers, each monomeric unit has a *dualistic character*; that is, repeating polymer unit, which is usually considered as a structureless bead, actually incorporates both repulsive and attractive parts concurrently. Indeed, a large number of macromolecules possess a pronounced amphiphilicity in every repeat unit.[27] Typical examples are synthetic polymers like poly(styrene sulfonate), poly(4-vinylpyridine), poly(1-vinylimidazole), poly(*N*-isopropylacrylamide), poly(2-ethyl acrylic acid), *etc.* In each repeat unit of such polymers there are hydrophilic (polar) and hydrophobic (non-polar) atomic groups, which have different affinity to the surrounding medium.[27] Many of the amino acids also contain both polar and non-polar groups simultaneously and, strictly speaking, the interaction between such amino acid residues in proteins cannot be literally reduced to pure hydrophilic or pure hydrophobic site–site interactions, as it is presupposed in the standard polymer field-theoretic models by discarding all details of side-group interactions. Other important biopolymers—polysaccharides, phospholipids—are also typical amphiphiles. Moreover, among the synthetic polymers, polyamphiphiles are very close to biological macromolecules in nature and behavior. In principle, they may provide useful analogs of proteins and are important for modeling some fundamental properties and sophisticated functions of biopolymers such as protein folding, formation of secondary structures, and enzymatic activity. Understanding the physics of self-assembly of the copolymers with dualistic monomer–monomer interaction is extremely challenging and also important because the underlying ideas have found connections to other fundamental areas, *e.g.*, phase transitions in membranes, crumpled surfaces, and geometry of random surfaces.

In this paper we study the effect of local polymer structure by introducing two coarse-grained conformationally asymmetric linear copolymer models with a local structural asymmetry, one of a comb-tail (CT) type (Fig. 1) and another we call "continuous jackknife (JK) model" (Fig. 2) The copolymers consist of amphiphilic and "monophilic" (non-amphiphilic) blocks, which have different segmental volume and tend to segregate into subphases due to the dualistic character of monomer–monomer interaction. Using a SCFT framework, we will explore the morphologies and phase diagrams for these model copolymers

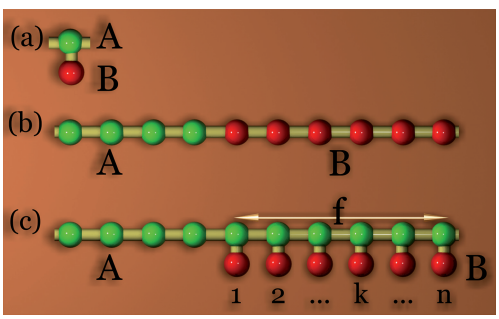

Fig. 1 Architecture of the diblock copolymers: (a) amphiphilic AB monomer unit, (b) conventional AB diblock copolymer, (c) amphiphilic CT diblock copolymer.

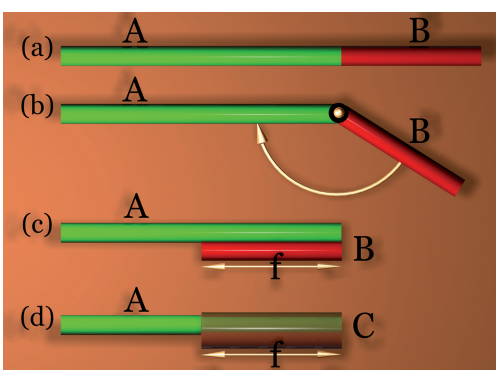

Fig. 2 Jackknife (JK) model of an amphiphilic diblock copolymer: (a) conventional linear AB diblock copolymer, (b) and (c) rotation of the shorter section B around the crankshaft connecting the A and B sections, (d) conformationally asymmetric AC diblock copolymer with A units of the segmental volume v and C units of the segmental volume $2v$.

and compare them with that known for conventional, conformationally symmetric diblock copolymers.

In the literature, there are several coarse-grained polymer models in which spherical (bead-like) monomers are replaced by composite asymmetric objects.[28,29] Generally, this gets a host of qualitatively new structures, *e.g.*, liquid crystalline phases of helical secondary structures.[29] One of the possible simplest variants is the hydrophobic-amphiphilic HA *side chain model* introduced in ref. 30–33 (for a review, see ref. 28 and 34). In this model, there are two main ingredients: chain units are connected to each other in a linear fashion and each amphiphilic unit of the chain possesses a spatial direction representing the local direction associated with the chain. Familiar examples in protein science include the exotic models that treat the protein backbone not as a chain of spheres but as a chain of anisotropic objects (*e.g.*, such as coins) for which one of the three directions differs from the other two. If such a chain is viewed as being made up of stacked coins instead of tethered spheres, we naturally arrive at the picture of an elastic tube (like a garden hose or spaghetti) whose axis coincides with the chain backbone.[29] At this coarse-grained level of description, new physics arises from the interplay between two length scales: the range of (anisotropic and many-body) attractive interactions and the thickness of the tube.[29]

The rest of the paper is organized as follows. The models of copolymers with an amphiphilic segment are described in the next section. The results are presented and discussed in Section 3. Concluding remarks are given in Section 4. All the technical details related to the SCFT and some additional data from our calculations are collected in the Appendix.

2. Models of diblock copolymers with amphiphilic segment

The comb-tail (CT) model

An amphiphilic diblock copolymer consists of a "monophilic" homopolymer block A and an amphiphilic block. In terms of graph theory, the amphiphilic part of the CT macromolecule can be modeled as a "caterpillar graph" rather than a linear graph corresponding to the standard "two-letter" Gaussian model. Namely, we refer to an **AB** graph in which the set {**A**} represents the nodes in the backbone and the set {**B**} the so-called legs connected by bridges (Fig. 1c) as a caterpillar of a given length. There are n legs, which are assumed to be distributed regularly along the backbone chain consisting of m sites. Each backbone node corresponds to a monophilic group (*e.g.*, CH_2–CH group) whereas the leg is considered as a single-site side group attached to the node. With this representation, each amphiphilic unit is treated as a two-site AB "dumbbell" or "dipole" consisting of A and B sites linked together (Fig. 1c). The monomeric units A and B are assumed to be of equal volume v. The two sites in the "dumbbell" are repelling each other so that the amphiphilic unit prefers to be at the A/B boundary rather than in A- or B-bulk, *i.e.*, this unit possesses a significant *surface activity*.

As shown earlier by some of us,[30,31] this fact can lead to a completely different self-organization of globules made of amphiphilic copolymers. In this paper we show that the microphase separation in melt of diblock copolymer chains schematically depicted in Fig. 1c (homopolymer A tail linked to a block of AB dumbbells) differs significantly from that in the melt of usual diblock copolymer chains shown in Fig. 1b. Because of the specific architecture of the copolymer, we expect that the microphase separation can in principle occur at two different length scales,[35–39] either "between" the linear homopolymer A tail and the composite AB amphiphilic section or "inside" the AB amphiphilic block. In the former case, the behavior should generally resemble that of a conventional diblock copolymer, where two blocks are incompatible homopolymers.

The main parameters governing the phase behavior of the CT model are defined as follows. The length fraction of amphiphilic AB segments, denoted below by letter C, is f, and the length fraction of monomers belonging to the homopolymer tail A is $1 - f$. Therefore, the volume fractions of A and B interaction sites, f_A and f_B, are

$$f_A = (1 + f)^{-1}, f_B = f(1 + f)^{-1} \quad (1)$$

The fractions f, f_A, and f_B can be expressed *via* the numbers of the monophilic (m) and amphiphilic (n) monomer units as follows:

$$f = n(m + n)^{-1}, f_A = (m + n)(m + 2n)^{-1}, f_B = n(m + 2n)^{-1} \quad (2)$$

It is assumed that M identical copolymer chains, each consisting of $N = N_A + N_B$ chemically bonded segments with equal segment volumes $v_A = v_B = v$ are densely packed into the volume $V = MNv$. It is clear that the conformational asymmetry of the CT model is due to the difference in volumes occupied by monophilic (A) and amphiphilic (C) units as well as to the fact that the architecture of the comb-like block is not invariant under the interchange of A monomers with B monomers. The A and B units are assumed to be incompatible, the degree of incompatibility being characterized by the conventional Flory–Huggins parameter $\chi = \chi_{AB}$.

It should be noted that our CT model is quite similar to that used by Nap and ten Brinke[35,36] and Khalatur and Khokhlov[40] who studied the self-organization of comb-shaped copolymers in the weak segregation regime.

The jackknife (JK) model

The continuous monophilic/amphiphilic copolymer model, which looks like a jackknife (JK model), is schematically depicted in Fig. 2. The JK copolymer can be obtained by the transformation of a linear AB copolymer of the contour length L consisting of two parts A and B, whose contour lengths are L_A and L_B ($L = L_A + L_B$, $L_A > L_B$), respectively (Fig. 2a). It is assumed that the chain sections of A and B type are characterized by the same Kuhn segment length ℓ and the same segmental volumes $v_A = v_B = v$. We rotate the shorter section B around the crankshaft connecting the A and B sections (Fig. 2b), fold it with the main chain (Fig. 2c) and then merge the two sections (Fig. 2d). This transformation leads to a new copolymer consisting of the homopolymer block A of length $L_A = L - L_B$ and the composite ("grey") block of type C with length $L_C = L_B$ and segmental volume $2v$. Therefore, the conformational asymmetry parameter[22] $\varepsilon = v_C\ell_A^2/v_A\ell_C^2$ of the resulting copolymer is $\varepsilon = 2$. In this model, each amphiphilic unit can be viewed as an analogue

of a point dipole. The length fraction f of the amphiphilic block is defined *via* $f_A = L_A/L$ as

$$f = f_A^{-1} - 1 \tag{3}$$

In the SCFT calculations carried out in this work, the JK copolymer is represented as a continuous curve and the probability distribution function for the chain length $L_{AC} = L_A$ to have its ends at points $\mathbf{r}$ and $\mathbf{r}'$ is given by the Edwards path integral[41] that depends on the position vector $\mathbf{r}[s]$ of the arc length variable s, s running from 0 to L_A. In what follows we set $L = 1$ so that $L_A = f_A$, and $s \in [0, f_A]$.

On the contrary, for the CT model, the contour variable s changes in the range $0 \le s \le s_1$ for monophilic tail, in the range $0 \le s \le s_2$ for k^{th} side-chain, and in the range $0 \le s \le s_3$ for bridge between k^{th} and $(k + 1)^{th}$ side-chains, where

$$s_1 = \frac{1-f}{1+f},\ s_2 = \frac{f}{n(1+f)},\ s_3 = \frac{f}{(n-1)(1+f)} \tag{4}$$

and $k = 1, 2, \ldots, n$; n being the number of side-chains (Fig. 1c). The sum of all sub-chain lengths in the CT model is $s_1 + ns_2 + (n - 1)s_3 = 1$. If the structural fragments of the CT model are measured in s_2 units, the monophilic chain's length is m, the comb-tail backbone's length is n, and the total length of all sub-chains is $N = m + 2n$.

The peculiarity of the JK model is that it is isomorphous (see Appendix) to the model of the diblock copolymer melt with conformational asymmetry.[22] On the other hand, the JK model is the limiting case of the CT model if the number of side chains $n \to \infty$, while the length fraction f is fixed. Now, the advantage of the CT model is that it allows for the internal structure of the systems under study. Thus, comparing the properties calculated for these two models we can estimate how much they are determined by the very fact of the conformational asymmetry of the amphipilic block copolymer melts (*i.e.* the fact that the composite amphiphilic units have doubled segment volume as compared to that of monophilic ones) and to which extent they are influenced by the presence of the internal structure of the amphiphilic units.

The phase behavior of the described amphiphilic copolymer systems is controlled by the overall degree of polymerization, N, the length fraction of the amphiphilic block, f, and the Flory–Huggins interaction parameter, χ, or, more precisely, the product $\tilde{\chi} = \chi N$. Depending on the values of $\tilde{\chi}$ and f, various states are expected to become stable in such systems ranging between a homogeneous (disordered) state at low values of $\tilde{\chi}$ and various ordered morphologies at higher $\tilde{\chi}$, the order–disorder and order–order transitions being separated by these regimes. In the next section we investigate the order–disorder and order–order transitions (ODT and OOT) and build the corresponding phase diagrams for the model amphiphilic copolymers in the plane $(f,\tilde{\chi})$. We examine the two models described above and compare them to simple conformationally symmetric linear diblocks, focusing on differences and similarities between the amphiphilic and monophilic copolymers. The polymer segment density profiles $\varphi_\alpha(\mathbf{r})$ (α = A, B), whose symmetry allows to distinguish between different morphologies, are calculated numerically *via* the SCFT method modified for the CT and JK models as described in Appendix.

3. Results and discussion

3.1. "Direct" and "inverse" morphologies

Since the amphiphilic C block consists of two incompatible species A and B attached closely to each other, the microphase separation in such melts is expected to involve the following two processes: (i) the segregation of amphiphilic C blocks as a whole from monophilic A blocks and (ii) the segregation of A units from B units inside amphiphilic C blocks. Obviously, the second process is not possible for the continuous JK model. In this subsection we focus on the first process and start with the discussion of the microphase separation observed for the simplest JK model.

It is well known that the majority and minority components of simple linear diblocks in the melt state form a matrix and spherical or cylindrical micelles, respectively.[1–9] We refer to such conventional morphologies as the "direct" ones. Since the continuous JK polymer is, in fact, equivalent to a simple A_{1-f}-b-C_f diblock, its majority block A(C) is also expected to form the matrix whereas its minority block C(A) should be located in micelles. However, there are two important distinctions between the conventional monophilic (Fig. 1a) and amphiphilic block copolymers: (i) each amphiphilic C segment occupies double volume as compared to that for a monophilic segment and (ii) the C segment has a composite (A + B) structure. Besides, the B component is always the minority component for the nonzero length of the monophilic tail A. Due to these distinctions a new type of "inverse" morphologies appears in amphiphilic block copolymers. To describe such inverse morphologies we visualize them in Fig. 3 where the 3D distribution of the local volume fraction of the B segments, $\varphi_B(\mathbf{r})$, is built for the incompressible melt of amphiphilic chains at various values of $\tilde{\chi}$ and f. The regions rich in A and B components are shown in blue and red, respectively; intermediate regions are given in yellow and green (see the color map).

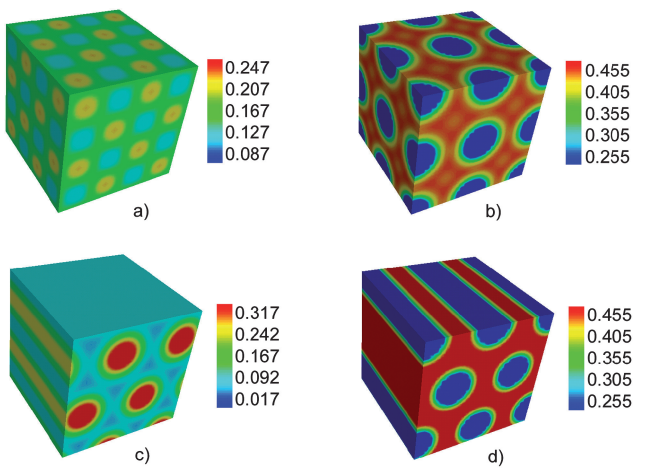

Fig. 3 Direct [(a) and (c), $f = 0.20$] and inverse [(b) and (d) $f = 0.55$] morphologies for the JK model. The 3D distribution of the volume fraction $\varphi_B(\mathbf{r})$ of the minority B component is shown for direct BCC [(a), $\chi N = 50.5$] and HEX symmetry [(c), $\chi N = 55$] as well as for the inverse BCC [(b), $\chi N = 65$] and HEX [(d), $\chi N = 80$] symmetry.

As seen in Fig. 3, for the chosen values of $\tilde{\chi}$ and f the SCFT predicts the well-known 3D body-centered-cubic (BCC) and 2D hexagonal (HEX) morphologies. If the B-fraction is sufficiently low ($f = 0.2$ or $f_B = 1/6$), the conventional direct morphologies are formed. In these morphologies the minority B-units are concentrated (together with the A-units the B-units are linked to), depending on the value of $\tilde{\chi}$, within the spherical (for the BCC) or cylindrical (for the HEX) micelles surrounded by the majority A matrix. On the contrary, if the fraction of B units is not too low ($f = 0.55$ and $f_B = 11/31$), then the A-units are concentrated within the micelles whereas the B-units (together with the A-units the B-units are linked to) form the matrix. In other words, the majority A phase turns out to be surrounded by the minority B phase. Further we refer to such morphologies as the "inverse" ones. The formation of the "direct" and "inverse" morphologies is also observed for the CT model (see Fig. 4 for some typical examples).

At the first glance, the existence of the inverse morphologies is a purely geometric phenomenon resulting from the very fact that the amphiphilic C units are composite. Indeed, in the presented examples of the inversed morphologies the length fraction of the monophilic units A is $1 - f$. So, it seems to be no surprise that the shorter monophilic block tends to concentrate within the micelles.

However, the presence of the conformational asymmetry makes the situation less trivial. Namely, an increase in the conformational asymmetry leads to a decrease in the critical value of the amphiphilic block average volume fraction that demarcates the direct and inverse morphologies. In particular, for the JK model the SCFT results in the following estimate of the critical point: $f_{cr} = 0.275$ and $\chi N = 43.1$. Substituting f_{cr} in eqn (1) and taking into account that the average volume fraction of amphiphilic units is $2f_B$, we find that in this point both the length and volume fractions of the monophilic tail ($f^{length}_{mono} = 0.725$ and $f^{vol}_{mono} = 0.569$, respectively) are larger than 1/2. Thus, the conformational asymmetry noticeably favors the appearance of inversed structures. It means that the amphiphilic monomer units are much more predisposed to form micelles rather than monophilic ones.

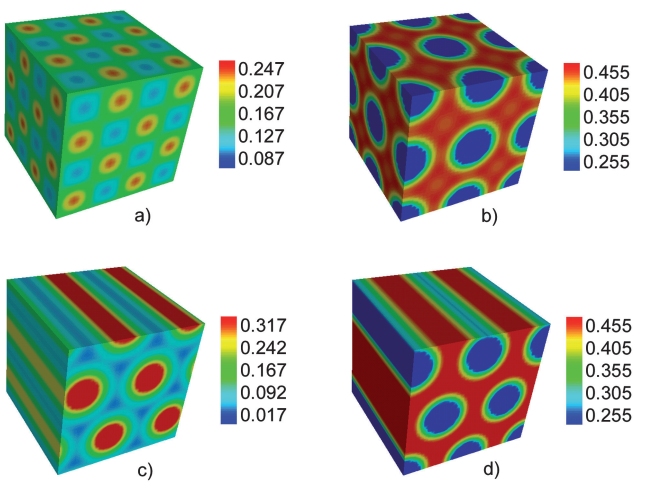

Fig. 4 Direct [(a) and (c), $f = 0.20$, $m = 16$, $n = 4$] and inverse [(b) and (d) $f = 0.55$, $m = 9$, $n = 11$] morphologies for the CT model. The 3D distribution of the volume fraction $\varphi_B(\mathbf{r})$ of the minority B component is shown for direct BCC [(a), $\chi N = 58.8$] and HEX symmetry [(c), $\chi N = 65$] as well as for the inverse BCC [(b), $\chi N = 75$] and HEX [(d), $\chi N = 80$] symmetry.

3.2. Phase diagrams

To study the phase behavior of the amphiphilic block copolymers under consideration we calculated and compared the free energies of the lamellar (LAM), hexagonal (HEX), gyroid (G), body centered cubic (BCC), and face centered cubic (FCC) morphologies for various compositions f within the interval $40 \leq \tilde{\chi} \leq 90$.[42] The phase diagrams for both models studied are presented in Fig. 5 in the plane $(f,\tilde{\chi})$. Taking into account that in the CT model the number of side-chains is integer, we depict the predicted phase diagrams as bar graphs with the corresponding discrete values f.

Both phase diagrams look basically similar. To properly interpret the differences between the phase diagrams we should remember (see discussion in section 2) that both models similarly describe those features of the amphiphilic block copolymer melts, which are determined mostly by the very fact of the conformational asymmetry, whereas the properties influenced by the presence of the internal structure of the amphiphilic units are taken into account by the CT model only.

First, both phase diagrams are rather asymmetric. Indeed, the lamellar phase is stable preferably in the half-plane $f < 1/3$. Moreover, the LAM morphology becomes equilibrium (for not too high value of $\tilde{\chi} \geq 80$) even in the rather asymmetric case $f = 0.2$, which is noticeably beyond the composition interval, where the LAM phase stays stable (even for high values of $\tilde{\chi}$) for the conventional symmetric block copolymers. On the contrary, the

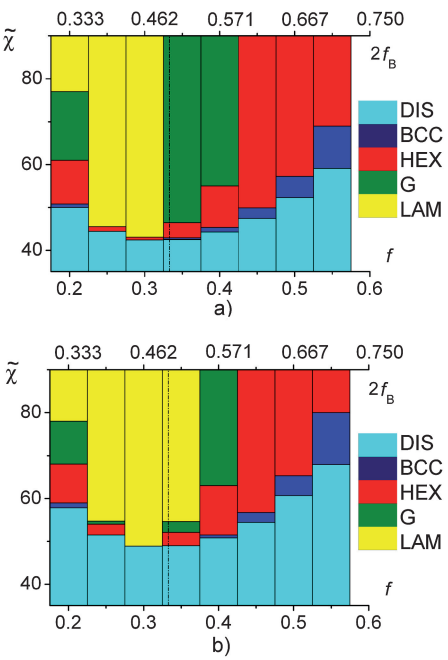

Fig. 5 Phase diagrams for amphiphilic diblock copolymer melts: (a) the JK model, (b) the CT model. The colored bars show the stable morphology: LAM is given in yellow, BCC in blue, HEX in red, G in green, and disorder in light-sea-green.

regions, where the BCC, HEX and G phases are stable, are located in the half-plane $f > 1/3$. Such an asymmetry is closely related to the conformational asymmetry of the amphiphilic block copolymers. As already mentioned in section 2, the conformational asymmetry in the SCFT[22] is described by the parameter $\varepsilon = v_A\ell_B^2/v_B\ell_A^2$. Therefore, the same phase diagram would correspond to two systems, which differ at the molecular level: (a) $\ell_A = \ell_B$, $v_A = \varepsilon v_B$ and (b) $\ell_B^2 = \varepsilon\ell_A^2$, $v_A = v_B$. It enables us to compare our phase diagram calculated for the amphiphilic copolymer melt within the JK model (isomorphous to the conformationally asymmetric block copolymer melt with $\varepsilon = 2$) with that of the asymmetric block copolymer melt with a numerically close value of $\varepsilon = 2.25$ calculated by Matsen and Bates[24] (see Fig. 5a). It is seen that our phase diagram for the JK model does look as a discrete version of that for a conformationally asymmetric diblock copolymer melt with a close value of the asymmetry parameter ε. In particular, the JK critical point coordinates recalculated in the variables of ref. 24 are $f_A = 0.569$ and $\chi N = 10.8$, which is pretty close to the corresponding values taken from Fig. 2b of ref. 24.

Now, comparing the phase diagrams shown in Fig. 5a and 5b we see that the existence of an internal structure taken into account by the CT model only results in two main effects. First, the phase transition lines for the CT amphiphilic copolymers are shifted upwards in comparison to those for the JK melt. This fact agrees with the general concept that the more complex the polymer melts are, the more stable the disordered phase is. In other words, the ODT shifts to lower temperatures as compared to the ODT of diblock copolymer melts. The reason is quite obvious: the more complex copolymers lose relatively more entropy under structure formation. Second, the presence of an internal structure leads to a minor smearing of the asymmetry composition effect in favor of the LAM phase. Besides, the region of the gyroid phase stability close to the critical point becomes somewhat broader.

Summarizing, the phase behavior of the amphiphilic block copolymers for not too incompatible blocks is most determined by their conformational asymmetry whereas the temperature (or $\tilde{\chi}$) values of the OOT at high $\tilde{\chi}$ are strongly influenced by the internal structure of the amphiphilic units.

3.3. Domain spacings

There exist rather noticeable internal structure effects, which are clearly revealed in formation of the so-called structure-in-structure (S-in-S) morphologies, which were earlier observed in the *two-length-scale* multiblock copolymer systems.[13–16] For amphiphilic systems, the S-in-S morphologies arise due to the presence of two characteristic length scales, one of which is just the Kuhn length ℓ separating the A and B units (somewhat incompatible), whereas the second length is the periodicity D of the ordered stable morphology.

To describe the two-scale structure formation in amphiphilic block copolymer melts in more detail, we are to determine not only its symmetry but also the dependence of the domain spacing D on the $\tilde{\chi}$-parameter. It is this dependence which distinguishes the peculiarities of microphase separation in CT and JK models for high values of $\tilde{\chi}$ (strong incompatibility). Indeed, in Fig. 6 we plotted the domain spacing D measured in

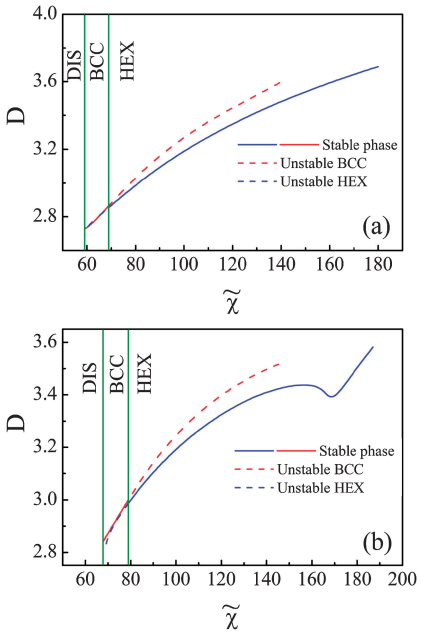

Fig. 6 Morphology periods D measured in units of the diblock copolymer gyration radius at $f = 0.55$. The vertical lines demarcate the stability regions for different phases. The bold solid lines correspond to the stable BCC (red line) and HEX (blue line) morphologies, the dashed lines do to the metastable ones. (a) The JK model and (b) the CT model ($m = 9$ and $n = 11$).

the units of the gyration radius of the diblock copolymer chain as a function of $\tilde{\chi}$.

For the JK model, which disregards the internal structure of amphiphilic units C, the $D(\tilde{\chi})$ function is a piecewise continuous (with some jumps in the OOT points) monotonously increasing function (see Fig. 6a), which is a typical behavior reflecting an overall increase of the chain stretching with increase of the blocks incompatibility.

For the CT model a new conformational change occurs within the HEX symmetry (see Fig. 6b): after passing a maximum at $\tilde{\chi} \sim 156$ the function $D(\tilde{\chi})$ drops down a bit and after passing a minimum at $\tilde{\chi} \sim 169$ increases again. Such a non-monotonic behavior, which was first found by Nap *et al.*[38] and then studied in more detail by Kriksin *et al.*[39] for the LAM phase, has been shown[38,39] to be an indicator of so-called lamellar-in-lamellar formation in multiblock copolymers with two-length-scale architecture. The latter is caused by starting of segregation inside of the shorter blocks with a characteristic scale L_S and requirement of commensurability between L_S and the overall periodicity D.

The fact that the 2D S-in-S does occur in amphiphilic block copolymers as well as the difference between the CT and JK models, which do and do not allow for the internal structure of the amphiphilic block copolymers, respectively, are clearly demonstrated in Fig. 7, where we presented the 2D profiles of the volume fraction $\varphi_B(\mathbf{r})$ for a $\tilde{\chi}$-value above the S-in-S onset for both the models.

4. Conclusion

In this paper we applied a properly modified SCFT procedure to study self-assembling (microphase separation) in amphiphilic

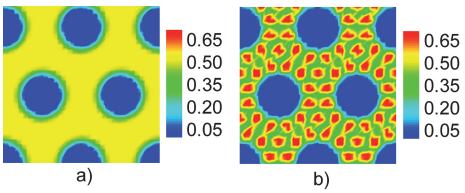

Fig. 7 Hexagonal morphology at $f = 0.55$ and $\chi N = 180$. The volume fraction $\varphi_B(\mathbf{r})$ of B monomer units: (a) the JK model and (b) the CT model ($m = 9$ and $n = 11$).

diblock copolymer melt. Therewith, to distinguish the effect of an internal structure of the amphiphilic units, we studied both the JK model, which treats the amphiphilic diblock copolymer as a sort of a conformationally asymmetric diblock copolymer without any internal structure and CT model, which directly takes into account this internal structure.

The modified SCFT equations were solved by the pseudo-spectral method and the phase diagrams for both models were calculated. The phase diagrams are considerably asymmetric, which is basically determined by the conformational asymmetry of the system under consideration, the composition behavior of the phase diagrams being in perfect agreement with the previous SCFT studies of the conformationally asymmetric diblock copolymer melts.[23–25] However, the presence of the internal structure of amphiphilic units results in a rather noticeable increase of stability of the low $\tilde{\chi}$ phases. Another important internal structure effect, which has been first studied in the present paper, is formation of the structure-in-structure pattern for the HEX symmetry, which is closely related to a non-monotonous behavior of the HEX structure periodicity D on the $\tilde{\chi}$-parameter.

Summarizing, we show that the effects related to the presence of an internal structure of the amphiphilic units are quite considerable for amphiphilic block copolymer melts with high incompatibility (see also ref. 32 and 33). The explicit accounting of the internal structure is crucial for the correct description of this important class of copolymers. Such dependence of the features of the microphase separation transition on the peculiarities of the local chemical structure of monomer units provides a new insight in the theory of microdomain structures in block copolymers.

SCFT procedure for amphiphilic copolymers

The free energy of an incompressible melt of flexible-chain AB copolymers reads[9]

$$F[\psi_A,\psi_B]/VT = V^{-1}\int d^3\mathbf{r}[-f_A\psi_A(\mathbf{r}) - (1-f_A)\psi_B(\mathbf{r}) + (\psi_A(\mathbf{r}) - \psi_B(\mathbf{r}))^2/(4\chi N)] - \ln Q[\psi_A,\psi_B] \quad (A1)$$

Here, V is the system volume, f_α is the average volume fraction of monomer units of type α (α = A, B; $f_A + f_B = 1$), χ is the Flory–Huggins parameter; N is the total polymerization degree, $\psi_\alpha(\mathbf{r})$ is the external field acting on the monomer unit of the α-th type located at the point $\mathbf{r}$, the temperature T is measured in the energetic units in which the Boltzman constant $k_B = 1$, and $Q[\psi_A,\psi_B]$ is the single-chain partition function to be defined below.

First, we describe the CT amphiphilic model in detail. To calculate the *single-chain* partition function $Q[\psi_A,\psi_B]$ appearing in eqn (A1) for this architecture, we divide our branching polymer chain (see Fig. 2c) into $2n$ elementary linear sub-chains: A-homopolymer tail, $(n-1)$ A-bridges between the sidechains, and n B-sidechains. Each sub-chain is described by two end-to-end segment distribution functions (direct and reverse functions, respectively): $q_f(\mathbf{r},s)$ and $q_b(\mathbf{r},s)$ for A-homopolymer tail ($0 \le s \le s_1$); $q_{3k-2}(\mathbf{r},s)$ and $q_0(\mathbf{r},s)$ for k-th sidechain ($0 \le s \le s_2$); $q_{3k-1}(\mathbf{r},s)$ and $q_{3k}(\mathbf{r},s)$ for the bridge between k-th and $(k+1)$-th sidechains, $0 \le s \le s_3$. The sub-chain lengths s_k ($k = 1,2,3$) were defined in eqn (4). All these functions satisfy the modified diffusion equation

$$\partial q(\mathbf{r},s)/\partial s = \nabla^2 q(\mathbf{r},s) - \psi_\alpha(\mathbf{r})q(\mathbf{r},s) \quad (A2)$$

with α = A for $q_f(\mathbf{r},s)$, $q_b(\mathbf{r},s)$, $q_{3k-1}(\mathbf{r},s)$, and $q_{3k}(\mathbf{r},s)$; α = B for $q_{3k-2}(\mathbf{r},s)$ and $q_0(\mathbf{r},s)$. The initial conditions are as follows:

$$q_f(\mathbf{r},0) = q_0(\mathbf{r},0) = 1,\ q_2(\mathbf{r},0) = q_f(\mathbf{r},s_1)q_0(\mathbf{r},s_2),\ q_{3k-1}(\mathbf{r},0) = q_{3k-4}(\mathbf{r},s_3)q_0(\mathbf{r},s_2)\ (k = 2,\ldots,n-1),\ q_{3n-3}(\mathbf{r},0) = q_0(\mathbf{r},s_2),\ q_{3n-2}(\mathbf{r},0) = q_{3n-4}(\mathbf{r},s_3),\ q_{3k-3}(\mathbf{r},0) = q_{3k}(\mathbf{r},s_3)q_0(\mathbf{r},s_2)\ (k = 2,\ldots,n-1),\ q_{3k-2}(\mathbf{r},0) = q_{3k-4}(\mathbf{r},s_3)q_{3k}(\mathbf{r},s_3)\ (k = 2,\ldots,n-1),\ q_b(\mathbf{r},0) = q_3(\mathbf{r},s_3)q_0(\mathbf{r},s_2),\ q_1(\mathbf{r},0) = q_f(\mathbf{r},s_1)q_3(\mathbf{r},s_3)$$

Now the single-chain partition function $Q[\psi_A,\psi_B]$ is defined by equation

$$Q[\psi_A,\psi_B] = V^{-1}\int d^3\mathbf{r}q_b(\mathbf{r},s_1). \quad (A3)$$

The local volume fractions $\varphi_A(\mathbf{r})$ and $\varphi_B(\mathbf{r})$ are defined as

$$\varphi_A(\mathbf{r}) = \frac{1}{Q[\psi_A,\psi_B]}\left[\int_0^{s_1} ds q_f(\mathbf{r},s)q_b(\mathbf{r},s_1-s) + \sum_{k=1}^{n-1}\int_0^{s_3} ds q_{3k-1}(\mathbf{r},s)q_{3k}(\mathbf{r},s_3-s)\right] \quad (A4)$$

$$\varphi_B(\mathbf{r}) = \frac{1}{Q[\psi_A,\psi_B]}\sum_{k=1}^{n}\int_0^{s_2} ds q_0(\mathbf{r},s)q_{3k-2}(\mathbf{r},s_2-s) \quad (A5)$$

where the functions $\psi_\alpha(\mathbf{r})$ and $\varphi_\alpha(\mathbf{r})$ (α = A, B) obey the SCFT equations

$$\psi_A(\mathbf{r}) = \chi N[\varphi_B(\mathbf{r}) - f_B] + \xi(\mathbf{r}),\quad \psi_B(\mathbf{r}) = \chi N[\varphi_A(\mathbf{r}) - f_A] + \xi(\mathbf{r}) \quad (A6)$$

$$\varphi_A(\mathbf{r}) + \varphi_B(\mathbf{r}) = 1,\ \xi(\mathbf{r}) = (\psi_A(\mathbf{r}) + \psi_B(\mathbf{r}))/2 \quad (A7)$$

Next, we describe the JK amphiphilic model (Fig. 3c). It can be considered as the limiting case and simplification of the CT model. Indeed, when the number of side chains $n \to \infty$, while the length fraction f is fixed, the distribution of B segments along the backbone becomes continuous. The segments of A type are subjected to the field $\psi_A(\mathbf{r})$, while the composite segments of AB (or C) type are subjected to the combined field $\psi_A(\mathbf{r}) + \psi_B(\mathbf{r})$. Therefore, for a given s, we have

$$\psi(\mathbf{r},s) = \begin{cases} \psi_A(\mathbf{r}), & 0 \le s < 2f_A - 1 \\ \psi_A(\mathbf{r}) + \psi_B(\mathbf{r}), & 2f_A - 1 \le s \le f_A \end{cases} \quad (A8)$$

where f_A has been defined by eqn (1).

The JK model single-chain partition function is given by

$$Q[\psi_A,\psi_B] = V^{-1}\int d^3\mathbf{r} q(\mathbf{r},f_A;[\psi_A,\psi_B]) \quad (A9)$$

where the end-to-end distribution function $q(\mathbf{r},s) = q(\mathbf{r},s;[\psi_A,\psi_B])$ is defined by the modified diffusion equation

$$\frac{\partial}{\partial s}q(\mathbf{r},s) = \nabla^2 q(\mathbf{r},s) - \psi(\mathbf{r},s)q(\mathbf{r},s), q(\mathbf{r},s) = 1 \quad (A10)$$

To calculate the local volume fractions we need the reverse end-to-end distribution function $q^+(\mathbf{r},s)$ satisfying the analogous equation

$$\frac{\partial}{\partial s}q^+(\mathbf{r},s) = \nabla^2 q^+(\mathbf{r},s) - \psi(\mathbf{r},s)q^+(\mathbf{r},f_A - s), q^+(\mathbf{r},s) = 1 \quad (A11)$$

The local volume fractions $\varphi_A(\mathbf{r})$ and $\varphi_B(\mathbf{r})$ are given by the integrals

$$\varphi_A(\mathbf{r}) = \frac{1}{Q(\psi_A,\psi_B)}\int_0^{f_A} ds q^+(\mathbf{r},f_A - s)q(\mathbf{r},s) \quad (A12)$$

$$\varphi_B(\mathbf{r}) = \frac{1}{Q(\psi_A,\psi_B)}\int_{2f_A-1}^{f_A} ds q^+(\mathbf{r},f_A - s)q(\mathbf{r},s) \quad (A13)$$

For the JK model, the fields $\psi_\alpha(\mathbf{r})$ and volume fractions $\varphi_\alpha(\mathbf{r})$ (α = A, B) also obey the SCFT eqn (A6), (A7).

Eqn (A2), (A10), and (A11) are solved with periodic boundary conditions which depends on the geometry of computational cell. The solution procedure is based on the pseudo-spectral method.[9,16] The free energy (A1) is to be minimized with respect to the dimensions of the simulation box.[16]

We show now that the JK model is isomorphous to the model of simple asymmetric AC diblock melt (Fig. 2d), where the segment A occupies the volume v and the homogeneous segment C occupies the double volume $2v$. To this end, we introduce the variables

$$\mu_A(\mathbf{r}) = \varphi_A(\mathbf{r}) - \varphi_B(\mathbf{r}), \mu_C(\mathbf{r}) = 2\varphi_B(\mathbf{r}) \quad (A14)$$

$$w_A(\mathbf{r}) = \psi_A(\mathbf{r}), w_C(\mathbf{r}) = [\psi_A(\mathbf{r}) + \psi_B(\mathbf{r})]/2 \quad (A15)$$

where $\mu_A(\mathbf{r})$ and $\mu_C(\mathbf{r})$ are the local volume fractions of the monophilic backbone A and the C chain segments at point $\mathbf{r}$ subjected to the fields $w_A(\mathbf{r})$ and $2w_C(\mathbf{r})$, respectively. The factor 2 arises due to the double volume of the segment C. From (A14) and (A15), we have

$$\varphi_A(\mathbf{r}) = \mu_A(\mathbf{r}) + \mu_C(\mathbf{r})/2, \varphi_B(\mathbf{r}) = \mu_C(\mathbf{r})/2 \quad (A16)$$

$$\psi_A(\mathbf{r}) = w_A(\mathbf{r}), \psi_B(\mathbf{r}) = 2w_C(\mathbf{r}) - w_A(\mathbf{r}) \quad (A17)$$

Next, after the substitution of eqn (A16) and (A17) in eqn (A6) and (A7) we obtain the SCFT equations with respect to new variables defined by (A14) and (A15)

$$\mu_A(\mathbf{r}) = \chi_{AC}N(\mu_C(\mathbf{r}) - 2f_B) + \xi_1(\mathbf{r}), \mu_C(\mathbf{r}) = \chi_{AC}N(\mu_A(\mathbf{r}) - 1 + 2f_B) + \xi_1(\mathbf{r}) \quad (A18)$$

$$\mu_A(\mathbf{r}) + \mu_C(\mathbf{r}) = 1, \xi_1(\mathbf{r}) = (w_A(\mathbf{r}) + w_C(\mathbf{r}))/2 \quad (A19)$$

where $\chi_{AC} = \chi/4$ characterizes the effective interaction between the block A and the composite block C.

Acknowledgements

This work was supported by the Deutsche Forschungsgemainschaft (SFB 569, project B13 "Smart copolymers near patterned substrate: Surface-modulated morphologies"), the Dutch Organization for scientific research NWO (Grant 047.016.002), Russian Foundation for Basic Research (Grant 07-03-00385) and Russian Federal Agency on Science and Innovations (contract 02.513.11.3329). We thank Yuliya Smirnova for useful discussion.

References

1 F. S. Bates and G. H. Fredrickson, *Annu. Rev. Phys. Chem.*, 1990, **41**, 525.
2 F. S. Bates and G. H. Fredrickson, *Phys. Today*, 1999, **33**, 32.
3 I. W. Hamley, *The Physics of Block Copolymers*, Oxford University Press, Oxford, 1998.
4 *Block Copolymers in Nanoscience*, ed. M. Lazzari, G. Liu and S. Lecommandoux, Wiley-VCH, 2006.
5 *Nanostructured Soft Matter. Experiment, Theory, Simulation and Perspectives. Series: NanoScience and Technology*, ed. A. V. Zvelindovsky, Springer, 2007.
6 L. Leibler, *Macromolecules*, 1980, **13**, 1602.
7 M. W. Matsen and M. Schick, *Phys. Rev. Lett.*, 1994, **72**, 2660.
8 M. W. Matsen and F. S. Bates, *Macromolecules*, 1996, **29**, 1091.
9 G. H. Fredrickson, *The Equilibrium Theory of Inhomogeneous Polymers*, Oxford University Press, 2006.
10 E. W. Cochran, C. J. Garcia-Cervera and G. H. Fredrickson, *Macromolecules*, 2006, **39**, 4264–4264.
11 N. Hadjichristidis, M. Pitsikalis, S. Pispas and H. Iatrou, *Chem. Rev.*, 2001, **101**, 3747.
12 B.-K. Cho, A. Jain, S. M. Gruner and U. Wiesner, *Science*, 2004, **305**, 1598.
13 R. Nap, C. Kok, G. ten Brinke and S. I. Kuchanov, *Eur. Phys. J. E*, 2001, **4**, 515.
14 Yu. G. Smirnova, G. ten Brinke and I. Ya. Erukhimovich, *J. Chem. Phys.*, 2006, **124**, 054907.
15 S. Kuchanov, V. Pichugin and G. ten Brinke, *Europhys. Lett.*, 2006, **76**, 959.
16 Yu. A. Kriksin, I. Ya. Erukhimovich, P. G. Khalatur, Yu. G. Smirnova and G. ten Brinke, *J. Chem. Phys.*, 2008, **128**, 244903.
17 I. Ya. Erukhimovich, *Eur. Phys. J. E*, 2005, **18**, 383.
18 J. Ruokolainen, R. Mäkinen, M. Torkkeli, T. Mäkelä, R. Serimaa, G. ten Brinke and O. Ikkala, *Science*, 1998, **280**, 557.
19 J. Ruokolainen, G. ten Brinke and O. T. Ikkala, *Adv. Mater.*, 1999, **11**, 777.
20 O. Ikkala and G. ten Brinke, *Science*, 2002, **295**, 2407.
21 O. Ikkala and G. ten Brinke, *Chem. Commun.*, 2004, 2131.
22 J. D. Vavasour and V. D. Witmore, *Macromolecules*, 1993, **26**, 7070.
23 M. W. Matsen and M. Schick, *Macromolecules*, 1994, **27**, 4014.
24 M. W. Matsen and F. S. Bates, *J. Polym. Sci., Part B: Polym. Phys.*, 1997, **35**, 945.
25 D. J. Pochan, S. P. Gido, J. Zhou, J. W. Mays, M. Whitmore and A. J. Ryan, *J. Polym. Sci., Part B: Polym. Phys.*, 1997, **35**, 2629–2643.
26 N. Zhou, T. P. Lodge and F. S. Bates, *J. Phys. Chem. B*, 2006, **110**, 3979–3989.
27 *Amphiphilic Block Copolymers: Self-assembly and Applications*, ed. P. Alexandridis and B. Lindman, Elsevier, Amsterdam, 2000.

28 P. G. Khalatur and A. R. Khokhlov, *Adv. Polym. Sci.*, 2006, **195**, 1–100.
29 J. R. Banavar and A. Maritan, *Rev. Modern Phys*, 2003, **75**, 23.
30 V. V. Vasilevskaya, P. G. Khalatur and A. R. Khokhlov, *Macromolecules*, 2003, **36**, 10103.
31 V. V. Vasilevskaya, A. A. Klochkov, A. A. Lazutin, P. G. Khalatur and A. R. Khokhlov, *Macromolecules*, 2004, **37**, 5444.
32 A. R. Khokhlov, Yu. A. Kriksin, I. Ya. Erukhimovich and P. G. Khalatur, *AIP Conf. Proc.*, 2007, **963**, 416.
33 A. R. Khokhlov and P. G. Khalatur, *Chem. Phys. Lett.*, 2008, **461**, 58.
34 A. R. Khokhlov and P. G. Khalatur, *Curr. Opin. Colloid Interface Sci.*, 2005, **10**, 22.
35 R. Nap, *Self-Assembling Block Copolymer Systems Involving Competing Length Scales*, PhD thesis, Rijksuniversiteit Groningen, 2003.
36 R. Nap and G. ten Brinke, *Macromolecules*, 2002, **35**, 952.
37 R. Nap, I. Ya. Erukhimovich and G. ten Brinke, *Macromolecules*, 2004, **37**, 4296.
38 R. Nap, N. Sushko, I. Ya. Erukhimovich and G. ten Brinke, *Macromolecules*, 2006, **39**, 6765.
39 Yu. A. Kriksin, I. Ya. Erukhimovich, Yu. G. Smirnova, P. G. Khalatur and G. ten Brinke, *J. Chem. Phys.*, 2009, **130**, 204901.
40 P. G. Khalatur and A. R. Khokhlov, *J. Chem. Phys.*, 2000, **112**, 4849.
41 M. Doi and S. F. Edwards, *The Theory of Polymer Dynamics*, Oxford Science Publications, Oxford, 1986.
42 Such a limited list of the assumed stable phases does not guarantee, of course, that all possible stable phases are explored. However, it includes the phases one observes most often and does not demand huge computational costs, thus providing a good insight concerning the amphiphilic block copolymer melts behavior, which is the main purpose of the present paper.

